Chapter 2

Mean field theory and the spinodal lines

In Chapter 1, we discussed the physical properties of reversible gel and the gelation of associating polymers. At the macroscopic level, reversible polymer gel is characterized by solid-like elasticity at high frequencies as well as liquid-like relaxations at long time scales. On the other hand, static inhomogeneities are frozen in the microscopic structures of the gel phase (Ikkai and Shibayama, 1999; Shibayama et al., 2000).

We noted that gelation in the solution of associating polymers is related to the microphase transition in copolymer systems. (For a discussion of experimental observations in diblock copolymer melts, see Chapter 3.) However, in contrast to the order-disorder transition, reversible gels do not have well-developed periodicity in the micro-structures. Therefore gelation to order-disorder transition resembles glass transition to crystallization; reversible gels share similar features as supercooled liquids, which exhibit non-equilibrium relaxations and breaking of ergodicity.

In this chapter we study the thermodynamics of the solution of A-B-A triblock copolymers, where the A monomers are associating. This system is the most widely studied model for reversible gelation (Tanaka and Matsuyama, 1989; Tanaka and Stockmayer, 1994; Ishida and Tanaka, 1997; Semenov et al., 1995a,b; Semenov and Rubinstein, 1998a,b). We adopt two mean-field approaches. First, density functional calculations can provide snapshots of the micro-structures of the solution under microphase transition. We hope to confirm our conjecture that across the microphase order-disorder transition, random structures with finite wave lengths are possible; such structures provide natural candidates for the gel phase[1]. Unfortunately we were not able to obtain enough numerical results to support our conjecture, therefore this part is only a summary of the theoretical model. Second, we construct the mean-field phase diagram through a quadratic expansion of the free energy (effective potential) from the Edwards Hamiltonian. The phase diagram shows both binodal coexistence

[1] Wolynes and co-workers (Singh et al., 1985; Hall and Wolynes, 1987) used density functional calculations to study the phase transition in an inhomogeneous hard-sphere liquid and found aperiodic structures as a more stable phase compared to the disordered liquid phase, which suggested aperiodic structures as natural candidates for the glass phase.

between polymer-rich and polymer-poor solution phases, and a spinodal transition associated with the microphase transition. Comparing the phase diagram to experimental observations by Tanaka et al. (1979), we may conclude that the gelation is an incomplete microphase transition which manifests the underlying spinodal instability. In Chapter 3 we further demonstrate that the competition between microscopic monomer interactions and this spinodal instability at a finite length scale comparable to the polymer size, results in a glass transition, which supports our conjecture that gelation is an alternative random microphase transition to the order-disorder transition. In addition, the glass transition lines approach the microphase spinodal in the mean field limit (as chain lengths go to infinite); this result underscores the close relationship between gelation and the mean-field microphase spinodal.

2.1 Self-consistent field theory

Since the successful predictions of the ordered structures in diblock copolymer melts (Matsen and Schick, 1994), self-consistent mean field theory has been widely used to study the phase diagrams in diblock and multi-block copolymer systems, and polymer blends. Many results are summarized in the reviews by Schmid (1998) and by Fredrickson et al. (2002). Further extensions such as the dynamic density functional theory by Fraaije et al. (1997) and Uneyama and Doi (2005) allow systematic studies of the phase separation kinetics in these systems.

Self-consistent field (SCF) theories approximate systems with many-body interactions as non-interacting particles under effective fields. The external fields are determined self-consistently from the microscopic Hamiltonian in a mean-field approximation. Since the order parameter is a density distribution or a function variable, density functional calculations enable us to sample the whole space of density distributions, in particular, to find the free energy minima with irregular microscopic structures. [See Fraaije et al. (1997), or the reviews, Schmid (1998) and Fredrickson et al. (2002), for examples of irregular morphologies.]

SCF provides a natural way to probe the microscopic structures of associating polymer solutions, which in many aspects are similar to copolymer melts. But applying it to polymer solutions needs some caution. Depending on the solvent selectivity and the concentration of polymer segments, the polymer chain can be significantly stretched or collapsed: in this scenario the random phase approximation underlying the SCF theory breaks down. However, at the gelation point, polymer chains overlap with each other, therefore the solution is in the semi-dilute or concentrated regime: the correlation length is much smaller than the chain size and concentration fluctuations only renormalize the microscopic "monomer size" and "monomer interactions"; at the level of polymer aggregates, we expect density distributions to look similar as in a mean-field theory, and qualitative features of the mean field theory should be preserved. In fact, SCF theory has been shown to be qualitatively

valid in phase diagram calculations even when significant chain stretching is observed (Almdal et al., 1990). In addition, as long as the polymer concentration is far away from the critical point, long-range density fluctuations are not important and mean field approximation is valid; an analysis of fluctuation effects in the spirit of Fredrickson and Helfand (1987) is presented in the next chapter.

2.1.1 Microscopic Hamiltonian of polymer mixtures

A continuum Gaussian chain with length N in an external field $V(\mathbf{r})$ is described by the Edwards Hamiltonian (Doi and Edwards, 1986)

$$h_0[\mathbf{R}(t)] = \frac{3k_{\mathrm{B}}T}{2Nb^2}\int_0^1 \left[\left(\frac{\partial \mathbf{R}(t)}{\partial t}\right)^2 + V(\mathbf{R}(t))\right] \mathrm{d}t \tag{2.1}$$

where $\mathbf{R}(t)$ maps the configuration of the polymer ($0 \le t \le 1$ is a parametrization of the polymer chain), and Nb^2 is mean square end-to-end distance.

To account for monomer interactions, we introduce the density operators $\hat{\phi}_\alpha(\mathbf{r})(\hat{\phi}_{\mathrm{A}}, \hat{\phi}_{\mathrm{B}}, \hat{\phi}_{\mathrm{S}})$

$$\begin{aligned} \hat{\phi}_{\mathrm{A,B}}(\mathbf{r}) &= \sum_{m=1}^{n_{\mathrm{p}}} \int_0^1 \delta\left(\mathbf{r} - \mathbf{R}_{\mathrm{m}}(t)\right) \delta_{\mathrm{A,B}}(t)\mathrm{d}t, \\ \hat{\phi}_{\mathrm{S}}(\mathbf{r}) &= \sum_{n=1}^{n_{\mathrm{s}}} \delta\left(\mathbf{r} - \mathbf{r}_n\right). \end{aligned} \tag{2.2}$$

Here $\mathbf{R}_{\mathrm{m}}$ labels the spatial conformation of the m-th polymer chain; $\mathbf{r}_{\mathrm{n}}$ is the position of the nth solvent molecule; $\delta_{\mathrm{A,B}}(t)$ is used to label the A or B block, e.g., $\delta_{\mathrm{A}}(t) = 1$ if the segment at t is A and $\delta_{\mathrm{B}}(t) = 1 - \delta_{\mathrm{A}}(t)$. The spatial positions of solvent molecules and polymer chains are completely described by $\{\mathbf{R}_{\mathrm{m}}(t), \mathbf{r}_{\mathrm{n}}\}$.

The two-body interactions are given by[2]

$$\sum_{\alpha\beta} \varepsilon_{\alpha\beta}\hat{\phi}_\alpha\hat{\phi}_\beta = \sum_{\alpha\neq\beta} \chi_{\alpha\beta}\hat{\phi}_\alpha\hat{\phi}_\beta + \frac{1}{2}(\varepsilon_{\mathrm{AA}}\hat{\phi}_{\mathrm{A}} + \varepsilon_{\mathrm{BB}}\hat{\phi}_{\mathrm{B}} + \varepsilon_{SS}\hat{\phi}_S), \tag{2.3}$$

where

$$\chi_{\alpha\beta} = \varepsilon_{\alpha\beta} - \frac{1}{2}\left(\varepsilon_{\alpha\alpha} + \varepsilon_{\beta\beta}\right).$$

The last term in (2.3) can be dropped as $\varepsilon_{\alpha\alpha}$ reflect constant shifts of the external fields, or self-energy contributions, which do not affect the interaction free energy.

Besides the two-body enthalpic interactions, we also need to account for the incompressibility or the excluded volume effect. Strict incompressibility can be inserted by adding a delta function (ρ is

[2]Here the summation is over each pair once.

the average bulk density),

$$\prod_{\mathbf{r}} \delta \left[\sum_{\alpha} \hat{\phi}_{\alpha}(\mathbf{r}) - \rho \right]$$

to the partition function. Alternatively, we can assume a virial expansion ("soft" incompressibility)

$$c_1 \hat{\phi}_{\mathrm{p}}^2 + c_2 \hat{\phi}_{\mathrm{p}}^3,$$

where $\hat{\phi}_{\mathrm{p}} = \hat{\phi}_{\mathrm{A}} + \hat{\phi}_{\mathrm{B}}$ is the total density of polymer segments, and c_1 and c_2 are positive constants.

The total Hamiltonian of the system is

$$\begin{aligned} \frac{H}{k_{\mathrm{B}}T} = \sum_{m=1}^{n_{\mathrm{p}}} \frac{3}{2Nb^2} \int_0^1 \left[\left(\frac{\partial \mathbf{R}_{\mathrm{m}}(t)}{\partial t} \right)^2 + V(\mathbf{R}_{\mathrm{m}}(t)) \right] \mathrm{d}t \\ + \frac{1}{k_{\mathrm{B}}T} \int \left[\sum_{\alpha\beta} \varepsilon_{\alpha\beta} \hat{\phi}_{\alpha}(\mathbf{r}) \hat{\phi}_{\beta}(\mathbf{r}) + c_1 \hat{\phi}_{\mathrm{p}}(\mathbf{r})^2 + c_2 \hat{\phi}_{\mathrm{p}}(\mathbf{r})^3 \right] \mathrm{d}\mathbf{r}. \end{aligned} \tag{2.4}$$

The strict incompressibility will result in an osmotic pressure term which we will discuss in the derivation of self-consistent equations.

2.1.2 Partition function and self-consistent equations

2.1.2.1 Partition function

In the canonical ensemble with n_{p} polymers and n_{s} solvent molecules, the classical partition function is ($\beta = 1/k_{\mathrm{B}}T$)

$$Z(n_{\mathrm{p}}, n_{\mathrm{s}}) = \int \mathcal{D}[\mathbf{R}_{\mathrm{m}}] \mathcal{D}[\mathbf{r}_{\mathrm{n}}] e^{-\beta H} \prod_{\mathbf{r}} \delta \left[\hat{\phi}_{\mathrm{A}}(\mathbf{r}) + \hat{\phi}_{\mathrm{B}}(\mathbf{r}) + \hat{\phi}_{\mathrm{S}}(\mathbf{r}) - \rho \right]. \tag{2.5}$$

Here $\mathcal{D}$ stands for functional integration (or path integral) over the configurations. And in a grand canonical ensemble where the chemical potential of polymer chains and solvents are given by μ_{p} and μ_{s}, we have[3]

$$\Xi(\mu_{\mathrm{p}}, \mu_{\mathrm{s}}) = \sum_{n_{\mathrm{p}}=0}^{\infty} \sum_{n_{\mathrm{s}}=0}^{\infty} \frac{\exp(\beta \mu_{\mathrm{p}} n_{\mathrm{p}} + \beta \mu_{\mathrm{s}} n_{\mathrm{s}})}{n_{\mathrm{s}}! n_{\mathrm{p}}!} Z(n_{\mathrm{p}}, n_{\mathrm{s}}). \tag{2.6}$$

To proceed, we introduce collective variables (functions) $\phi_{\alpha}(\mathbf{r})$, their conjugate fields $W_{\alpha}(\mathbf{r})$, and an osmotic pressure $\Pi(\mathbf{r})$ to get rid of the operator fields $\hat{\phi}_{\alpha}$. Insert

$$\int \mathcal{D}\phi_{\alpha} \delta(\phi_{\alpha} - \hat{\phi}_{\alpha}) \propto \int \mathcal{D}\phi_{\alpha} \int \mathcal{D}W_{\alpha} \exp\left[iW_{\alpha} \left(\phi_{\alpha} - \hat{\phi}_{\alpha} \right) \right] = \text{const.}$$

[3] In Wood and Wang (2002) the chemical potential of the polymer segments is assumed instead of that of the polymer chains.

into the partition function, we get

$$Z(n_{\rm p},n_{\rm s})=\frac{1}{\mathcal{N}}\int\mathcal{D}\phi_\alpha\int\mathcal{D}W_\alpha\int\mathcal{D}\Pi\exp\left\{-\beta H_1[\phi_\alpha]+iW_\alpha\phi_\alpha+i\int\Pi(\mathbf{r})\left[\sum_\alpha\phi_\alpha(\mathbf{r})-\rho\right]\mathrm{d}\mathbf{r}\right\}$$
$$\int\mathcal{D}\left[\mathbf{R}_{\rm m}\right]\int\mathcal{D}\left[\mathbf{r}_n\right]\exp\left\{-\beta H_0[\mathbf{R}_{\rm m},\mathbf{r}_{\rm n}]-iW_\alpha\hat{\phi}_\alpha\right\} \tag{2.7}$$
$$=\mathcal{N}^{-1}\int\mathcal{D}\phi_\alpha\exp\left[-\beta H_1(\phi_\alpha)-\beta F_0(\phi_\alpha)\right]; \tag{2.8}$$
$$\beta F_0(\phi_\alpha)=-\ln\int\mathcal{D}W_\alpha\mathcal{D}\Pi\exp\left\{iW_\alpha\phi_\alpha+i\int\Pi(\mathbf{r})\left[\sum_\alpha\phi_\alpha(\mathbf{r})-\rho\right]\mathrm{d}\mathbf{r}\right\}Z[iW_\alpha]; \tag{2.9}$$
$$Z[iW_\alpha]=\int\mathcal{D}\left[\mathbf{R}_{\rm m}\right]\int\mathcal{D}\left[\mathbf{r}_n\right]\exp\left\{-\beta H_0[\mathbf{R}_{\rm m},\mathbf{r}_{\rm n}]-iW_\alpha\hat{\phi}_\alpha\right\}=e^{-G_0(W_\alpha)} \tag{2.10}$$

where repeated indices imply integration over space, as well as summations over the same index,

$$W_\alpha\hat{\phi}_\alpha=\sum_\alpha\int W_\alpha(\mathbf{r})\hat{\phi}_\alpha(\mathbf{r})\mathrm{d}\mathbf{r}.$$

Physically ϕ_α and W_α correspond to the density distributions and their conjugate external fields, like the magnetic moment and the magnetic field, or the volume and the pressure in the liquid-gas system. $Z[iW_\alpha]$ gives the partition function of the imaginary system of non-interacting molecules under external fields iW_α (the imaginary unit i is introduced only for mathematical convenience), G_0 is the Gibbs free energy of this imaginary system, and F_0 is its Legendre transform, or the Helmholtz free energy in terms of the density fields ϕ_α.

$Z[iW_\alpha]$ can be calculated for arbitrary polymer systems using the random phase approximations. See Leibler (1980), Ohta and Kawasaki (1986), and de la Cruz (1991). $F_0[\phi_\alpha]$ can be expanded as a power series of ϕ_α, and the physical free energy $F=-\ln Z$ can in principle be calculated perturbatively. In the next section we shall derive the expansion of F up to quadratic order.

We note that in general the random phase approximation that assumes polymer chains to be ideal does not apply to polymer solutions as the polymer chains are swollen. Therefore our model applies to associating A-B-A polymers in a theta solvent for the middle block B, and a poor solvent for end block A. Alternatively we can interpret microscopic parameters as renormalized by chain swelling.

2.1.2.2 Self-consistent equations

In this section we derive the self-consistent equations from a saddle point approximation for the partition function in (2.7). Minimizing the exponential term with respect to ϕ_α, W_α, and Π we have

$$\frac{\delta}{\delta\phi_{\rm A}\left(\mathbf{r}\right)},\frac{\delta}{\delta\phi_{\rm B}\left(\mathbf{r}\right)},\frac{\delta}{\delta\phi_{\rm S}\left(\mathbf{r}\right)}=0\quad\Rightarrow$$

$$iW_{\mathrm{A}}(\mathbf{r})+i\Pi(\mathbf{r})=\beta\left[\varepsilon_{\mathrm{AB}}\phi_{\mathrm{B}}(\mathbf{r})+\varepsilon_{\mathrm{AS}}\phi_{\mathrm{S}}(\mathbf{r})+\varepsilon_{\mathrm{AA}}\phi_{\mathrm{A}}(\mathbf{r})+2c_1\phi_{\mathrm{p}}(\mathbf{r})+3c_2\phi_{\mathrm{p}}^2(\mathbf{r})\right]; \tag{2.11a}$$

$$iW_{\mathrm{B}}(\mathbf{r})+i\Pi(\mathbf{r})=\beta\left[\varepsilon_{\mathrm{AB}}\phi_{\mathrm{A}}(\mathbf{r})+\varepsilon_{\mathrm{BS}}\phi_{\mathrm{S}}(\mathbf{r})+\varepsilon_{\mathrm{BB}}\phi_{\mathrm{B}}(\mathbf{r})+2c_1\phi_{\mathrm{p}}(\mathbf{r})+3c_2\phi_{\mathrm{p}}^2(\mathbf{r})\right]; \tag{2.11b}$$

$$iW_{\mathrm{S}}(\mathbf{r})+i\Pi(\mathbf{r})=\beta\left[\varepsilon_{\mathrm{AS}}\phi_{\mathrm{A}}(\mathbf{r})+\varepsilon_{\mathrm{BS}}\phi_{\mathrm{B}}(\mathbf{r})+\varepsilon_{\mathrm{SS}}\phi_{\mathrm{S}}(\mathbf{r})\right]; \tag{2.11c}$$

$$\frac{\delta}{\delta\Pi\left(\mathbf{r}\right)}=0\Rightarrow\phi_{\mathrm{A}}\left(\mathbf{r}\right)+\phi_{\mathrm{B}}\left(\mathbf{r}\right)+\phi_{\mathrm{S}}\left(\mathbf{r}\right)=\rho; \tag{2.11d}$$

$$\frac{\delta}{\delta W_{\mathrm{S}}\left(\mathbf{r}\right)}=0\Rightarrow i\phi_{\mathrm{S}}\left(\mathbf{r}\right)=-\frac{\delta\ln Z(iW_\alpha)}{\delta W_{\mathrm{S}}(\mathbf{r})}; \tag{2.11e}$$

$$\frac{\delta}{\delta W_{\mathrm{A}}\left(\mathbf{r}\right)},\frac{\delta}{\delta W_{\mathrm{B}}\left(\mathbf{r}\right)}=0\Rightarrow i\phi_{\mathrm{A,B}}\left(\mathbf{r}\right)=-\frac{\delta\ln Z(iW_\alpha)}{\delta W_{\mathrm{A,B}}(\mathbf{r})}. \tag{2.11f}$$

To complete the set of equations we need to evaluate the partition function

$$Z(iW_\alpha)=Z_{\mathrm{p}}(iW_{\mathrm{A}},iW_{\mathrm{B}})\cdot Z_{\mathrm{s}}(iW_{\mathrm{S}}).$$

For solvent molecules we neglect their internal degrees of freedom,

$$Z_{\mathrm{s}}(iW_{\mathrm{S}})=\int\mathcal{D}[\mathbf{r}_{\mathrm{n}}]_{n=1,2,\cdots n_{\mathrm{s}}}\exp\left[-i\int W_{\mathrm{S}}\left(\mathbf{r}\right)\hat{\phi}_{\mathrm{S}}\left(\mathbf{r}\right)\mathrm{d}\mathbf{r}\right]=q_{\mathrm{s}}^{n_{\mathrm{s}}}, \tag{2.12}$$

where

$$q_{\mathrm{s}}=\int\exp\left[-iW_{\mathrm{S}}(\mathbf{r})\right]\mathrm{d}\mathbf{r}.$$

For polymer chains

$$Z_{\mathrm{p}}(iW_{\mathrm{A}},iW_{\mathrm{B}})=q_{\mathrm{p}}^{n_{\mathrm{p}}}, \tag{2.13}$$

where q_{p} is the partition function of a single polymer chain in external fields W_α. Details of the derivations of Z_{p} and its derivatives w.r.t. W_α are given in Appendix 2.A.1.

The self-consistent equations are

$$W_{\mathrm{A}}\left(\mathbf{r}\right)=\beta\left(\varepsilon_{\mathrm{AA}}\phi_{\mathrm{A}}+\varepsilon_{\mathrm{AB}}\phi_{\mathrm{B}}+\varepsilon_{\mathrm{AS}}\phi_{\mathrm{S}}+2c_1\phi_{\mathrm{p}}+3c_2\phi_{\mathrm{p}}^2\right), \tag{2.14a}$$

$$W_{\mathrm{B}}\left(\mathbf{r}\right)=\beta\left(\varepsilon_{\mathrm{BB}}\phi_{\mathrm{B}}+\varepsilon_{\mathrm{AB}}\phi_{\mathrm{A}}+\varepsilon_{\mathrm{BS}}\phi_{\mathrm{S}}+2c_1\phi_{\mathrm{p}}+3c_2\phi_{\mathrm{p}}^2\right), \tag{2.14b}$$

$$W_{\mathrm{S}}\left(\mathbf{r}\right)=\beta\left(\varepsilon_{\mathrm{SS}}\phi_{\mathrm{S}}+\varepsilon_{\mathrm{AS}}\phi_{\mathrm{A}}+\varepsilon_{\mathrm{BS}}\phi_{\mathrm{B}}\right); \tag{2.14c}$$

$$\phi_{\mathrm{S}}\left(\mathbf{r}\right)=n_s\left[\int\exp(-W_{\mathrm{S}}(\mathbf{r}))\mathrm{d}\mathbf{r}\right]^{-1}\exp\left(-W_{\mathrm{S}}\right), \tag{2.14d}$$

$$\phi_{\mathrm{A}}\left(\mathbf{r}\right)=Nn_{\mathrm{p}}\left[\int q(\mathbf{r},1)\mathrm{d}\mathbf{r}\right]^{-1}\int_0^1\theta_{\mathrm{A}}(t)q\left(\mathbf{r},t\right)q^*\left(\mathbf{r},1-t\right)\mathrm{d}t, \tag{2.14e}$$

$$\phi_{\mathrm{S}}\left(\mathbf{r}\right)=Nn_{\mathrm{p}}\left[\int q(\mathbf{r},1)\mathrm{d}\mathbf{r}\right]^{-1}\int_0^1\theta_{\mathrm{B}}\left(t\right)q\left(\mathbf{r},t\right)q^*\left(\mathbf{r},1-t\right)\mathrm{d}t; \tag{2.14f}$$

where $\phi_{\mathrm{p}}=\phi_{\mathrm{A}}+\phi_{\mathrm{B}}$, N is total the number of segments in each chain[4], and n_{p} and n_{s} are the

[4]For convenience we have assumed the monomer volume to be b^3.

number of polymer chains and solvent molecules, respectively. q and q^* are the once-integrated Green's functions to be obtained from solving the following diffusion equations

$$\left(\frac{\partial}{\partial t} - \frac{Nb^2}{6}\nabla^2_{\mathbf{r}} + N\sum_\alpha \theta_\alpha(t)\, W_\alpha(\mathbf{r})\right) q(\mathbf{r},t) = 0, \tag{2.15}$$

$$\left(\frac{\partial}{\partial t} - \frac{Nb^2}{6}\nabla^2_{\mathbf{r}} + N\sum_\alpha \theta_\alpha(1-t)\, W_\alpha(\mathbf{r})\right) q^*(\mathbf{r},t) = 0, \tag{2.16}$$

$$q(\mathbf{r},0) = q^*(\mathbf{r},0) = 1.$$

$\theta_\alpha(t)$ are labels for the different blocks. For a triblock copolymer with the structure $10A-80B-10A$, $\theta_\alpha(t)$ is defined as

$$\theta_{\mathrm{A}}(t) = \begin{cases} 1 & 0 \le t \le 0.1 \text{ or } 0.9 \le t \le 1 \\ 0 & 0.1 < t < 0.9 \end{cases} \tag{2.17}$$

$$\theta_{\mathrm{B}}(t) = 1 - \theta_{\mathrm{A}}(t).$$

The diffusion equations can be solved using the Crank-Nicholson scheme or the spectral method, as explained in Appendix 2.A.

2.2 Free energy expansion

In Section 2.1.1 we write the Hamiltonian of the polymer system and by introducing collective fields ϕ_α and W_α we get the free energy functions $G_0(W_\alpha)$ and $F_0(\phi_\alpha)$, as in Eqs. (2.10) and (2.9). Here we derive the perturbative expansion of F_0 and G_0 as a power series of the ϕ_α and W_α. From the quadratic term we find the mean field spinodal transition lines from the Helmholtz free energy F_0. The higher-order terms (many-body interactions) are necessary if we want to study the effects of fluctuations.

First we calculate $G_0(W_\alpha)$. From now on we replace iW_α by W_α. Note that

$$G_0(W_\alpha) = -k_{\mathrm{B}}T \ln Z(W_\alpha) = -\frac{1}{\beta}\ln \int \mathcal{D}\hat{\phi}_\alpha \exp\left(-\beta H_0 - W_\alpha \hat{\phi}_\alpha\right), \tag{2.18}$$

which admits an expansion into power series of W_α and connected correlation functions:

$$\begin{aligned} G_0(W_\alpha) - G_0(W_\alpha = 0) &= -\frac{1}{\beta}\sum_m \frac{1}{m!}\int \mathrm{d}\mathbf{x}_1 \mathrm{d}\mathbf{x}_2 \cdots \mathrm{d}\mathbf{x}_{\mathrm{m}} \\ &\quad \sum_\alpha G^{(\mathrm{m})}_{\alpha_1\alpha_2\cdots\alpha_{\mathrm{m}}}(\mathbf{x}_1,\mathbf{x}_2,\cdots,\mathbf{x}_{\mathrm{m}}) W_{\alpha_1}(\mathbf{x}_1) W_{\alpha_2}(\mathbf{x}_2)\cdots W_{\alpha_{\mathrm{m}}}(\mathbf{x}_{\mathrm{m}}) \\ &= -\frac{1}{\beta}\sum_{\mathrm{m}} \frac{1}{\mathrm{m}!} G_{\alpha_1\alpha_2\cdots\alpha_{\mathrm{m}}} W_{\alpha_1} W_{\alpha_2}\cdots W_{\alpha_{\mathrm{m}}}. \end{aligned} \tag{2.19}$$

From now on we will adopt the summation convention with integration over space.

The connected correlation functions $G^{(\mathrm{m})}$

$$G_c^{(\mathrm{m})}(\mathbf{x}_1,\mathbf{x}_2,\cdots,\mathbf{x}_\mathrm{n}) = \left.\frac{(-1)^\mathrm{m}\beta\delta^\mathrm{m}G_0(W_\alpha)}{\delta W(\mathbf{x}_1)\delta W(\mathbf{x}_2)\cdots\delta W(\mathbf{x}_\mathrm{n})}\right|_{W_\alpha=0} = \left\langle\hat{\phi}(\mathbf{x}_1)\hat{\phi}(\mathbf{x}_2)\cdots\hat{\phi}(\mathbf{x}_\mathrm{m})\right\rangle_c \tag{2.20}$$

can be calculated using the propagator of Gaussian chains; details are given in Appendix 2.B.1.

$F_0(\phi_\alpha)$ is the Legendre transform of $G_0(W_\alpha)$, which satisfies

$$F_0(\phi_\alpha) - G_0(W_\alpha) = -\frac{1}{\beta}\phi_\alpha W_\alpha = -\frac{1}{\beta}\int \phi_\alpha(\mathbf{x})W_\alpha(\mathbf{x})\mathrm{d}\mathbf{x}, \tag{2.21}$$

where ϕ_α are the averages of operators $\hat{\phi}_\alpha$ under external fields W_α, defined as

$$\phi_\alpha = \frac{\beta\delta G_0(W_\alpha)}{\delta W_\alpha} = \left\langle\hat{\phi}_\alpha\right\rangle_{W_\alpha}, \tag{2.22}$$

and we have

$$W_\alpha = -\frac{\beta\delta F_0(\phi_\alpha)}{\delta\phi_\alpha}. \tag{2.23}$$

It is known that in the expansion of $F_0(\phi_\alpha)$,

$$F_0(\varphi_\alpha+\bar{\phi}_\alpha) - F_0(\bar{\phi}_\alpha) = \frac{1}{\beta}\sum_{\mathrm{m}>1}\Gamma^{(\mathrm{m})}_{\alpha_1\alpha_2\cdots\alpha_\mathrm{m}}\varphi_{\alpha_1}\varphi_{\alpha_2}\cdots\varphi_{\alpha_\mathrm{m}}, \tag{2.24}$$

the vertex functions are related to the *amputated* connected correlation functions (Zinn-Justin, 2002):

$$\Gamma^{(2)}_{\alpha\beta}(\mathbf{x}_1,\mathbf{x}_2) = S_{\alpha\beta}(\mathbf{x}_1,\mathbf{x}_2) = \left[G_c^{(2)}(\mathbf{x}_1,\mathbf{x}_2)\right]^{-1}_{\alpha\beta}; \tag{2.25a}$$

$$\Gamma^{(3)}_{\alpha\beta\gamma}(\mathbf{x}_1,\mathbf{x}_2,\mathbf{x}_3) = -G^{(3)}_{\mathrm{amp}}(\mathbf{x}_1,\mathbf{x}_2,\mathbf{x}_3); \tag{2.25b}$$

$$\Gamma^{(4)}_{\alpha\beta\gamma\delta}(\mathbf{x}_1,\mathbf{x}_2,\mathbf{x}_3,\mathbf{x}_4) = -G^{(4)}_{\mathrm{amp}}(\mathbf{x}_1,\mathbf{x}_2,\mathbf{x}_3,\mathbf{x}_4) + \int G^{(3)}_{\mathrm{amp}}(\mathbf{x}_1,\mathbf{x}_2,\mathbf{y})G_c^{(2)}(\mathbf{y},\mathbf{z})G^{(3)}_{\mathrm{amp}}(\mathbf{z},\mathbf{x}_3,\mathbf{x}_4)\mathrm{d}\mathbf{y}\mathrm{d}\mathbf{z} + 2 \text{ permutations}; \tag{2.25c}$$

where

$$G^{(n)}_{\mathrm{amp}}(\mathbf{x}_1,\mathbf{x}_2,\cdots,\mathbf{x}_\mathrm{n}) = \int \mathrm{d}\mathbf{y}_1\mathrm{d}\mathbf{y}_2\cdots\mathrm{d}\mathbf{y}_n G^{(\mathrm{n})}_{\alpha'_1\alpha'_2\cdots\alpha'_\mathrm{n}}(\mathbf{y}_1,\mathbf{y}_2,\cdots\mathbf{y}_\mathrm{n}) S_{\alpha_1\alpha'_1}(\mathbf{x}_1,\mathbf{y}_1)S_{\alpha_2\alpha'_2}(\mathbf{x}_2,\mathbf{y}_2)\cdots S_{\alpha_\mathrm{n}\alpha'_\mathrm{n}}(\mathbf{x}_\mathrm{n},\mathbf{y}_\mathrm{n}). \tag{2.26}$$

The interacting free energy of the interacting system is

$$F(\phi) = H_1(\phi) + F_0(\phi). \tag{2.27}$$

At high temperatures ($\beta \ll 1$), the system is uniform and the free energy is minimized at $\phi = \bar{\phi}$. As the temperature decreases, the enthalpic interactions dominate over the entropic mixing term, and the system tends to phase separate. This is signaled by the instability at the quadratic expansion of the free energy with respect to perturbations of the order parameter $\varphi = \phi - \bar{\phi}$, i.e., the Hessian matrix attains negative eigen values. This defines the spinodal limit.

Up to quadratic order F is given by (See Appendix 2.B.2 for the derivation)

$$F^{(2)} = V \sum_{\mathbf{q}} \left[S^{-1}(q) - f(\beta\varepsilon) \right] \varphi_\alpha(\mathbf{q}) \varphi_\alpha(-\mathbf{q}) \tag{2.28}$$

where $S^{-1}(q)$ is the inverse structure factor, $\beta\varepsilon$ are the interaction parameters, $\varphi_\alpha(\mathbf{q})$ is the Fourier transform of $\varphi_\alpha(\mathbf{x})$, and φ_α^* is the complex conjugate of φ_α. $S^{-1}(q)$ is dependent on the chain composition and the bulk average volume fraction of polymers. To find the spinodal limit, we minimize $S^{-1}(q)$ and find the value $\beta\varepsilon$ such that $f(\beta\epsilon) \geq \min_q S^{-1}(q)$.

The wave vector q_m that minimizes $S^{-1}(q)$ gives the inverse of the correlation length of the phase separated structure. In the microphase transition, $q_\mathrm{m} \sim N^{-1/2}$, thus the correlation length is comparable to the chain length. In the macrophase phase separation, $q_\mathrm{m} = 0$. In the solution of associating triblock copolymers, both spinodals are present.

2.3 Results and discussion

First we look at the spinodal lines in the solution of associating triblock copolymers. For simplicity we assume that the only associating interaction is $\varepsilon_{\mathrm{AA}} = e_\mathrm{A} < 0$, the solvent molecules and B segments are assumed to be non-interacting.

In Figure 2.1 on page 20 we show the spinodal lines in the solution of associating polymers with composition 3A-4B-3A with different chain lengths: $N = 20, 40, 100$. The spinodal for the macrophase separation is shown in red, with a critical point; the spinodal for microphase transition is shown in blue. The phase diagram is very similar to the experimental results obtained for gelatin solution by Tanaka et al. (1979) and theoretical calculations by Tanaka (1989) and by Semenov and Rubinstein (1998a).

From Appendix 2.B.2 we find that the critical point in the binodal coexistence is given by

$$\frac{e_\mathrm{A}^*}{k_\mathrm{B}T} = \frac{1}{4f_\mathrm{A}^2(1-\phi_\mathrm{p})} + \frac{1}{4f_\mathrm{A}^2\phi_\mathrm{p}N},$$

which is of order $O(1)$, and the microphase spinodal satisfies $e_\mathrm{A} \sim N^{-1}$. Therefore increasing the chain length results in a large shift of the microphase spinodal, but only affects the macrophase spinodal weakly. The scaling $e \sim N^{-1}$ is also obtained by Tanaka et al. (1979) for the gelation line,

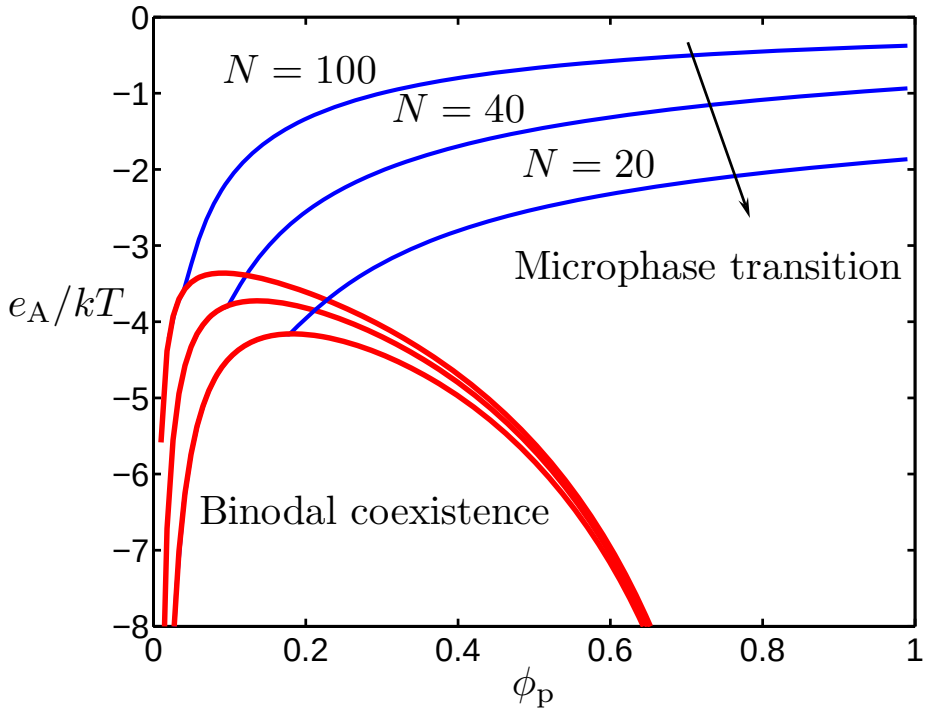

Figure 2.1: Spinodal lines for the microphase transition and the macrophase separation in solutions of associating polymers. The fraction of associating A block is 0.3 on each end of the triblock copolymer. Results are shown for associating polymers with three kuhn lengths ($N = 20$, $N = 40$ and $N = 100$). The red lines are the spinodal for the macrophase separation, with a critical point; the blue lines are the microphase spinodal with instability at wave vector $q_m > 0$.

while our result has no *a priori* assumption of the appearance of the gel phase. This coincidence suggests that gelation has the same thermodynamic signature as the microphase transition.

We notice that as chain length increases, the intersection point between the two spinodals is shifted to the left, suggesting that the solution is unstable with respect to the microphase transition for lower polymer concentrations. Therefore the solution of associating polymers with longer chains should form a gel at lower concentrations. This is expected both from the microscopic mechanism of self-assembly and from the thermodynamics of polymer solutions.

We also point out that the microphase spinodal does not terminate at the intersection, but continues below the binodal coexistence. Mathematically this implies a discontinuous jump in the quadratic coefficient a in the structure factor

$$S^{-1}(q) = q^4 - aq^2 + b.$$

This is different from the mean field Lifshitz point where a continuously decreases to zero. This might be an artifact of the mean field approximation, and fluctuation effects should drive the confluent

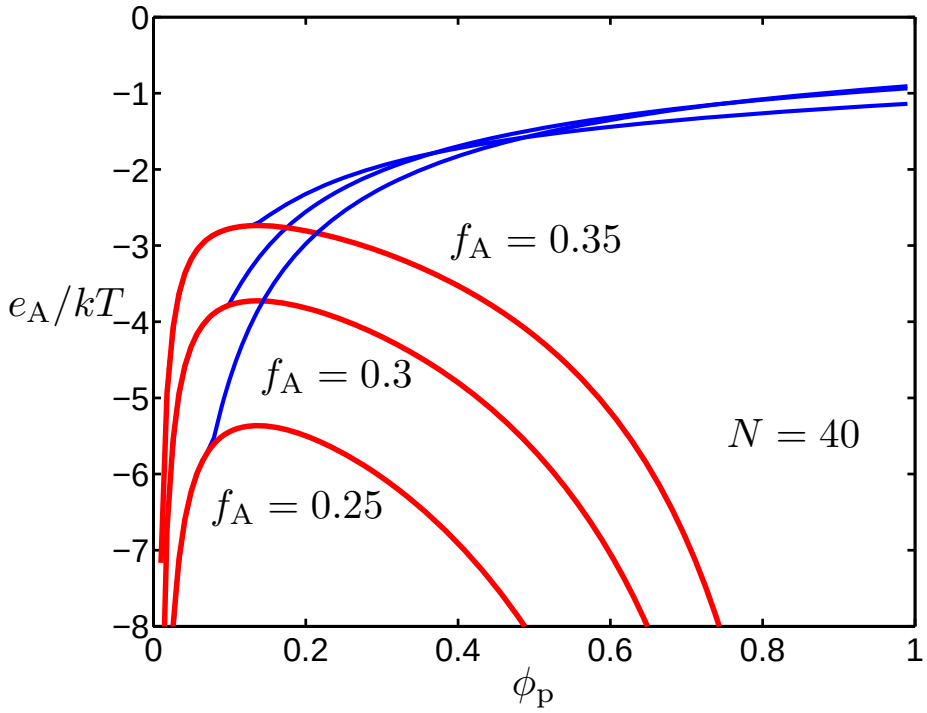

Figure 2.2: Spinodal lines in the solution of associating polymers with chain length $N = 40$ and different end-block fractions, $f_{\rm A} = 0.25, 0.3, 0.35$. The meaning of the curves are the same as in Fig. 2.1.

point to a Lifshitz tri-critical fixed point.

In Fig. 2.2 we plot the spinodal lines for associating polymers with fixed length ($N = 40$) at three different end-block fractions: $f_{\rm A} = 0.25, 0.3, 0.35$. Compared to Fig. 2.1 we see that increasing the end-block fraction has a big effect on the macrophase spinodal, but does not affect the microphase spinodal very much. This can be understood from the driving force for the phase transition in each case. In the macrophase separation, the driving force is mainly the enthalpic interactions, therefore increasing the fraction of A blocks can enhance the tendency for phase separation into A-rich and A-poor phases. On the other hand, for the microphase transition, the A blocks serve as connection while the B blocks are the linkers. Because of volume incompressibility, the local density of A segments is about the same for all chain compositions, therefore as long as the monomer interaction between A segments is strong enough, they will form aggregated structures dispersed in the B matrix. The driving force for this microphase transition is not only enthalpic, but also entropic, due to the presence of B linker. In fact, as shown in Figure 2.3 on page 22, if we further increase the end fraction to "unrealistic" high values $f_{\rm A} = 0.45$, we see that the microphase spinodal is shifted to even larger $e_{\rm A}$. In particular we observe that increasing the polymer concentration can dissolve the gel instead of triggering gelation as for lower end-block fractions. This corresponds to the "inversion" of the

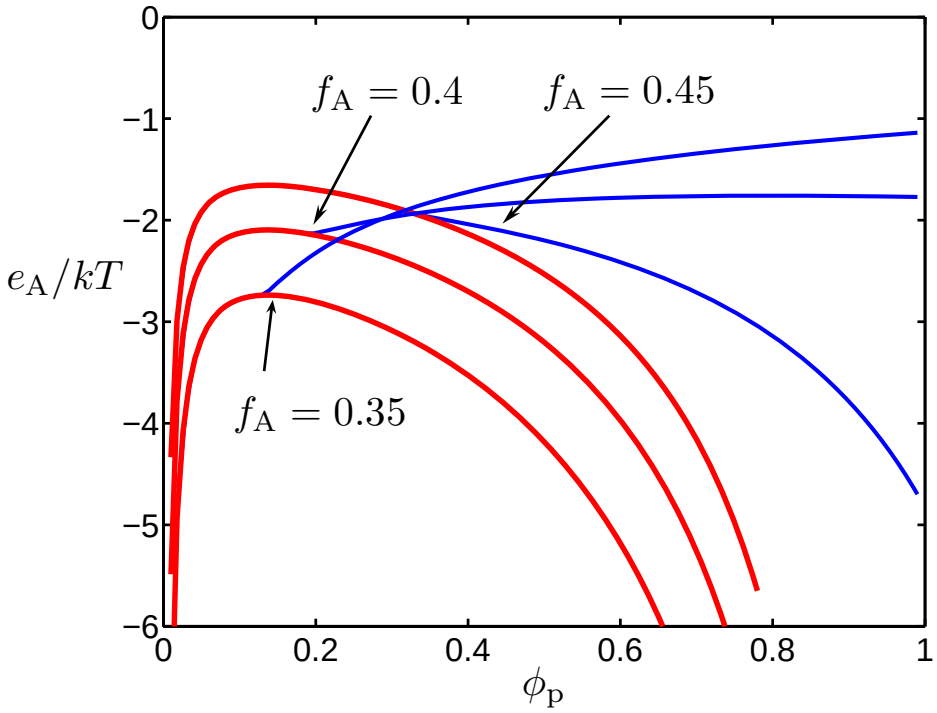

Figure 2.3: Spinodal lines in the solution of associating polymers with large end blocks. The chain length is $N = 40$ and results are shown for end fractions $f_A = 0.35, 0.4, 0.45$.

microphase structures from the A dispersed phase to the B dispersed phase, and clearly reflects the self-assembly nature of the transition.

We also note that for $f_A = 0.25$ the microphase spinodal intersects the binodal spinodal to the left of the critical point, implying the possibility of two co-existing microphases with different polymer concentrations. This is also found by Semenov and Rubinstein (1998a) for the gelation of associating polymers. Our results suggest that such a coexistence is due to the competition between short-range monomer interactions and the self-assembly of copolymers at the mesoscopic polymer length scale.

Figure 2.4 on page 23 shows the critical wave vector q_m associated with the microphase spinodal. The correlation length $\xi \sim q_m^{-1}$. From the two blue curves we see that for long chains or at high concentrations, the polymer chains are less swollen, as is expected from less screening. From the three curves with different compositions at $N = 40$ we see that the structure is more swollen for larger end-block fractions when the polymer concentration is high, but at low densities the trend is reversed. This probably reflects the entropic effect in the self-assembly, and can be easily tested in experimental measurements.

Finally in Figure 2.5 on page 24 we plot the microphase spinodal curves in a solution with virial

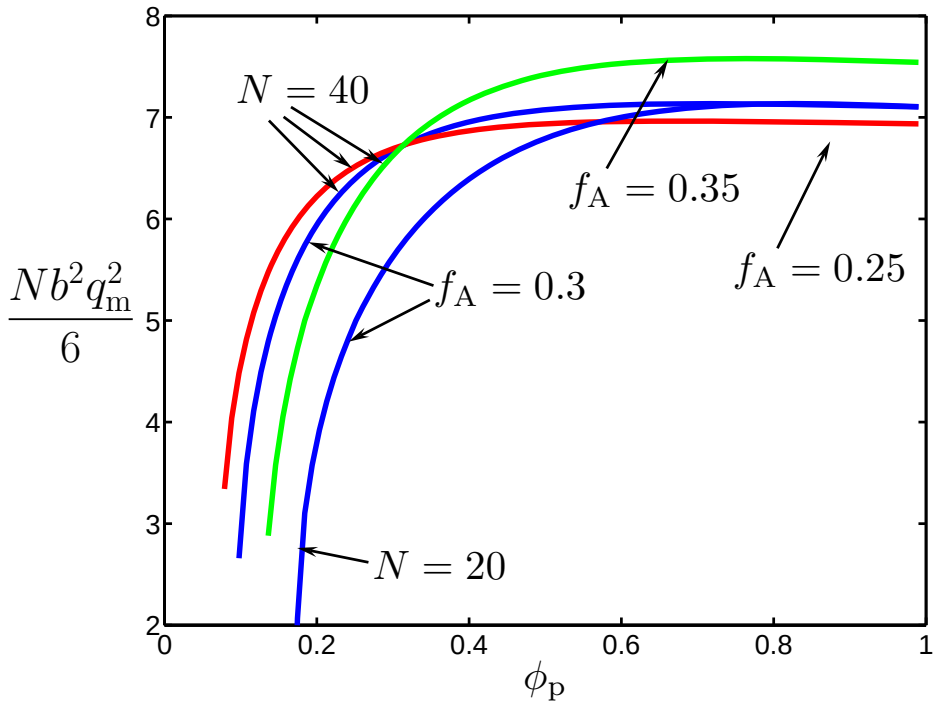

Figure 2.4: Critical wave vector in the solution of associating polymers. We present the results for three end block fractions, $f_{\rm A} = 0.25, 0.3, 0.35$ with chain length $N = 40$, and one curve $f_{\rm A} = 0.3$ for $N = 20$.

type expansion instead of volume incompressibility. The macrophase spinodals are not shown as they are similar to the previous cases. These results show similar features as for the model with strict volume incompressibility.

2.4 Conclusion

To summarize, from analysis of a simple system for reversible gelation—triblock associating polymer solutions—we find that such systems exhibit microphase transitions which share many similar features with the reversible gelation. We find that this transition is rather insensitive to the chain composition as compared to the chain length or associating energy. This reflects the nature of this transition, which is due to the interplay between short-range monomer aggregation and long-range polymer extension.

Although our work is carried out for triblock copolymer solutions, qualitative features should hold in other associating polymer systems, such as multi-block or even diblock copolymers: There should always be a microphase spinodal due to the segregation between A and B monomers. And these systems could exhibit gelation under certain conditions.

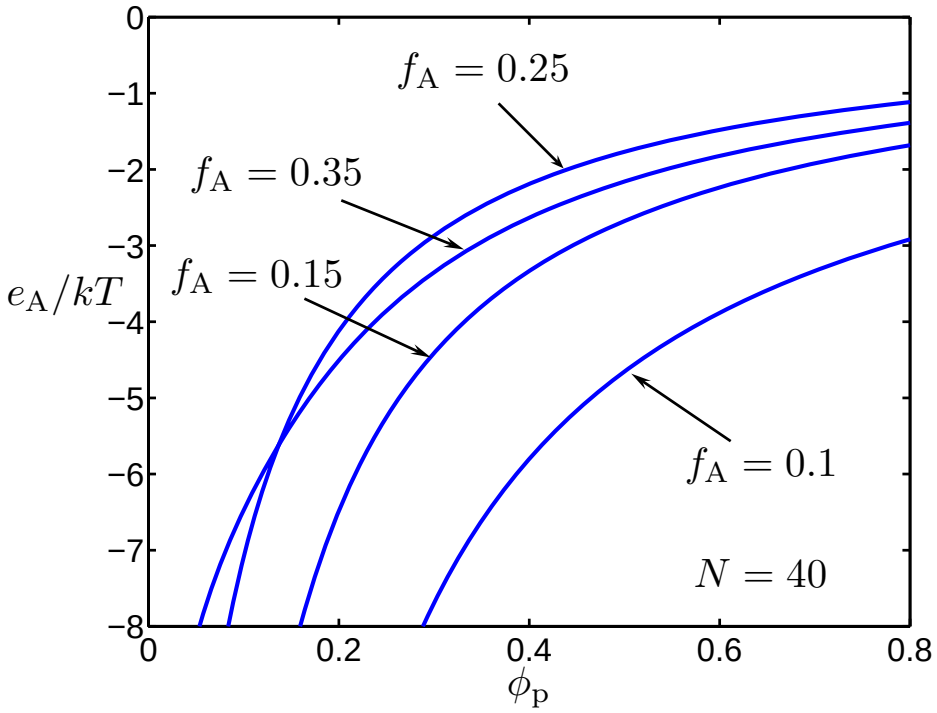

Figure 2.5: Microphase spinodal calculated using the virial-type expansion instead of strict volume incompressibility. The chain length is $N = 40$ with $c_1 = 1k_BT$ and $c_2 = 6k_BT$. Results are shown for $f_A = 0.1, 0.15, 0.25, 0.35$.

Our calculations suggest that one can start from the basic microscopic model to study the thermodynamics of gelation, without *a priori* assumptions of the gel phase. But the nature of reversible gelation, like the glass transition, is different from conventional phase transitions, and calls upon new theoretical tools. In the next chapter, which is adapted from our published paper, we analyze the possibility of glass transitions associated with this microscopic spinodal.

Appendix 2.A Self-consistent field calculation

2.A.1 Calculations of the partition functions of non-interacting polymers in external fields

In this subsection we solve the partition function $Z(iW_\alpha)$ as defined in Eq. (2.10). First we replace iW_α by W_α, it will turn out that thus defined W_α are real. From Eq. (2.12) we have

$$Z_s(iW_S) = \int \mathcal{D}[\mathbf{r}_n]_{n=1,2,\cdots n_s} \exp\left[-\int W_S(\mathbf{r})\,\hat{\phi}_S(\mathbf{r})\,d\mathbf{r}\right]$$